Materials Today Bio 11 (2021) 100112

Contents lists available at ScienceDirect

Materials Today Bio

journal homepage: www.journals.elsevier.com/materials-today-bio

Droplet microarrays for cell culture: effect of surface properties and nanoliter culture volume on global transcriptomic landscape

S. Chakraborty [a], V. Gourain [b], M. Benz [a], J.M. Scheiger [a,c], P.A. Levkin [a,d,**], A.A. Popova [a,*]

[a] Institute of Biological and Chemical Systems–Functional Molecular Systems (IBCS–FMS), Karlsruhe Institute of Technology (KIT), Hermann–von–Helmholtz–Platz 1, 76344 Eggenstein–Leopoldshafen, Germany
[b] Institute of Biological and Chemical Systems–Biological Information Processing (IBCS–BIP), Karlsruhe Institute of Technology (KIT), Hermann–von–Helmholtz–Platz 1, 76344 Eggenstein–Leopoldshafen, Germany
[c] Institute of Chemical Technology and Polymer Chemistry, Karlsruhe Institute of Technology (KIT), Engesserstr. 20, 76131 Karlsruhe, Germany
[d] Institute of Organic Chemistry, Karlsruhe Institute of Technology (KIT), Fritz-Haber Weg 6, 76131 Karlsruhe, Germany

ARTICLE INFO

Keywords:
Biomaterials
Cell–surface interaction
mRNA sequencing
Nanoliter volumes
Transcriptomic analysis

ABSTRACT

The development of novel chemically developed and physically defined surfaces and environments for cell culture and screening is important for various biological applications. The Droplet microarray (DMA) platform based on hydrophilic-superhydrophobic patterning enables high-throughput cellular screening in nanoliter volumes and on various biocompatible surfaces. Here we performed phenotypic and transcriptomic analysis of HeLa-CCL2 cells cultured on DMA, with a goal to analyze cellular response on different surfaces and culture volumes down to 3 nL, compared with conventional cell culture platforms. Our results indicate that cells cultured on four tested substrates: nanostructured nonpolymer, rough and smooth variants of poly(2-hydroxyethyl methacrylate-*co*-ethylene dimethacrylate) polymer and poly(thioether) dendrimer are compatible with cells grown in Petri dish. Cells cultured on nanostructured nonpolymer coating exhibited the closet transcriptomic resemblance to that of cells grown in Petri dish. Analysis of cells cultured in 100, 9, and 3 nL media droplets on DMA indicated that all but cells grown in 3 nL volumes had unperturbed viability with minimal alterations in the transcriptome compared with 96-well plate. Our findings demonstrate the applicability of DMA for cell-based assays and highlight the possibility of establishing regular cell culture on various biomaterial-coated substrates and in nanoliter volumes, along with routinely used cell culture platforms.

1. Introduction

Mammalian cell culture has revolutionized the field of biology since its conception in 1943, being an indispensable tool for basic biological research and clinical assays [1]. It enables researchers to control the physiological environment of cells and assess the downstream effects of various factors on cell biology [2,3]. The most important aspect of cell-based *in vitro* studies is the possibility of high-throughput screenings (HTS), which are crucial for fundamental research and drug development [4,5]. As demonstrated in a review by Swinney et al., 56% of the small-molecule drugs approved between 1999 and 2008 were discovered using cell-based phenotypic screenings [6]. To be able to culture cells *in vitro*, researchers need platforms that are compatible with cell culture and mimic at least partially the *in vivo* environment. In 1887, German physician Julius Petri initiated bacterial culture in nesting glass plates, which were later named after him as "Petri dishes" [7]. The modern Petri dishes for eukaryotic cell culture have evolved into plasma-treated polystyrene plates, where the surface turns hydrophilic once the cell culture medium is added and exhibits critical surface roughness necessary for attachment of adherent cells [8].

Cell–surface interactions are shown to have direct influence on the cellular growth, morphology, and behavior [9,10]. Both surface topography and chemistry were shown to be important criteria to ensure proper attachment and growth of cells on the substrate [11–13]. The development of novel, chemically and physically defined cell culture surfaces appropriate for a large variety of cell lines is crucial for modern biological research. Commonly used cell culture plates can be modified only to a certain extent by introducing different coatings or

* Corresponding author.
** Corresponding author. Karlsruhe Institute of Technology (KIT), Institute of Biological and Chemical Systems – Functional Molecular Systems (IBCS-FMS), Hermann-von-Helmholtz-Platz 1, 76344 Eggenstein-Leopoldshafen, Germany.
E-mail addresses: levkin@kit.edu (P.A. Levkin), anna.popova@kit.edu (A.A. Popova).

https://doi.org/10.1016/j.mtbio.2021.100112
Received 16 February 2021; Received in revised form 9 April 2021; Accepted 13 April 2021
Available online 30 April 2021

three-dimensional (3D) scaffolds. Therefore, researchers are keen to develop alternative platforms for cell culture to tune the culturing environment in terms of physical and chemical cues. Such cell culture platforms are often based on synthetic materials, biomaterials, and surfaces modified with various polypeptides or macromolecules such as fibronectin, laminin, matrigel, and others [14–17].

The need for performing large number of experiments to test multiple factors simultaneously led to the creation of microtiter plates, which may currently contain 6, 12, 24, 48, 96, 384, and 1536 wells and are widely used for cell-based screenings directed to fundamental research and drug discovery. There is a need for even higher throughput of biological experiments because of the growing demand for new medication and huge availability of natural and chemically synthesized compounds as possible drug candidates. On the other hand, it is necessary to increase physiological resemblance of cell-based experiments by using relevant cell lines such as primary and stem cells, which are limited in their availability. Therefore, there is a natural demand for further increase of throughput and decrease of cell consumption through miniaturization of culturing volumes. Commonly used microtiter plates are limited in the number of individual experiments to be performed and restricted to microliter culturing volumes, because they cannot be further miniaturized due to the capillary effects of the physical barriers forming the wells. Hence, there is a trend of developing alternative miniaturized cell culture platforms, most of which are based on microfluidic principle and allow testing of cells in picoliter to nanoliter volumes [18–20]. Microtiter plates are fairly considered as a reference point for newly developed cell culture platforms, since they were used for most of the *in vitro* experimental data generated till now. However, any cell culture platform is an artificial *in vitro* model, and with the development of alternative platforms for culturing and screening of live cells, it is important to understand how the cells differ in their biological state within different *in vitro* platforms [21,22].

We have previously introduced a novel cell culture platform named “Droplet microarray” (DMA) based on hydrophilic-superhydrophobic patterning, which allows the formation of wall-less arrays of separated nanoliter droplets [23]. This is an array of hydrophilic spots (of customizable shape and size) on a microscope glass slide divided by hydrophobic borders. It enables growing cells in the nanoliter-sized droplets to perform a wide range of high-throughput cell-based screenings [24,25]. In comparison to microtiter plates, DMA enables miniaturization of cell culture reservoirs down to nanoliter volumes due to the absence of solid walls used for liquid confinement, which create capillary effect upon miniaturization beyond a certain size. In order to create well-defined culturing conditions for different types of cells and applications, we use various types of surfaces and chemical modifications to fabricate the DMAs, all of which are tunable in terms of porosity, roughness, and chemical moiety.

In multiple previous studies we have demonstrated successful cell culture and high-throughput cellular screenings on DMA for a variety of cell types, such as HEK293 [23,24], HeLa [23,24], A549 [24], human embryonic stem cells (hESC) [25], HepG2 [26], Jurkat [27], mouse embryonic stem cells (mESC) [28], patient-derived chronic lymphocytic leukemia cells [29], MCF-7, MDA-MB-231, HCT116, HT-29, SK-OV-3, SK-MEL-28, PC-3, and hiPSCs (unpublished data). DMA can be used for two-dimensional (2D) monolayer or suspension cell culture, as well as for 3D cell culture models, such as spheroids [26,30]. The DMA platform is compatible with robotic liquid handlers, as well as automated microscopy and other read-out methods. This makes DMA a universal platform for a variety of cell-based assays, offering miniaturization of culturing volumes down to nanoliters and up to 2–30 times higher throughput comparing to microtiter plates.

The main goal of this work was to answer a question of whether the cells behave similar in commonly used microtiter plates and on DMAs fabricated with different surfaces and confined nanoliter volumes. Unprecedented landscape-scale understanding of any molecular response because of cell–substrate interactions can be best identified by investigating the cellular transcriptome [31]. Global transcriptome analysis was shown to have successfully annotated the effect of various substrate materials on altering the gene expression in a number of cell lines [32–36]. HeLa is an important human epithelial cancer cell line often used in regular cell culture and subsequent biomedical research [37]. The use of HeLa cells has been reported in approximately 60,000 research articles to date, including early discoveries such as the development of polio vaccine in 1952 [38], dissecting the link between human papillomavirus and cervical cancer, and studying the role of telomerase in preventing chromosomal degradation [39]. Moreover, whole genomic and transcriptomic landscapes of HeLa Kyoto cell line have been reported [40]. We used the original variant (HeLa-CCL2) of this extensively studied cell line for our research because these cells exhibit proper adherence to a diverse range of surface architecture. To gain detailed insights into cellular changes upon culturing on different surfaces and culturing volumes, our present study for the first time analyzes the changes in the transcriptome of HeLa-CCL2 cells grown on several biocompatible surfaces used for fabrication of DMAs, as well as in volumes ranging from 3 to 100 nL. Our results have shown that HeLa-CCL2 cells cultured on DMAs fabricated with various biomaterials and in nanoliter volumes (down to 9 nL) have comparable transcriptomic landscape compared with cells grown in traditional cell culture platforms, thereby highlighting the potential of DMA to be used as an alternate miniaturized platform for regular cell culture and high-throughput cell-based screenings.

2. Materials and methods

2.1. Materials and reagents

HeLa-CCL2 cells were purchased from DSMZ GmbH, Germany. Dulbecco's modified eagle medium, fetal bovine serum, penicillin-streptomycin solution, phosphate-buffered saline, bovine serum albumin, Hoechst 33342, Calcein AM, and propidium iodide were purchased from Life Technologies GmbH, Germany. Cellular mycoplasma contamination test kit was bought from PromoCell GmbH, Germany. Glutaraldehyde, hexamethyldisilazane (HMDS), paraformaldehyde, Triton X-100, Phalloidin-Atto 565 dye, and aqueous mounting medium were purchased from Sigma-Aldrich Chemie GmbH, Germany. RNeasy Mini kit was bought from QIAGEN GmbH, Germany. RNA chip and high-sensitivity DNA chips for Bioanalyzer were purchased from Agilent Technologies GmbH, Germany. TruSeq stranded messenger RNA (mRNA) kit was from Illumina GmbH, Germany. Standard microscope glass slides of 75 × 25 mm size and thin glass slides were from SCHOTT Technical Glass Solutions GmbH, Germany. Chemicals required for the fabrication of HEMA-EDMA polymer, poly(thioether) dendrimer coatings, and surface patterning were purchased from Sigma-Aldrich Chemie GmbH, Germany, and Merck Chemicals GmbH, Germany. Photomasks for surface patterning were bought from Rose Photomasken, Germany. Standard polystyrene Petri dishes (Catalog no. 664160, 100 mm diameter, 58 cm^2 growth area) and 96-well plates (Catalog no. 655180, 34 mm^2 growth area) for cell culture (sterile, with surface treatment for tissue culture) were purchased from Greiner Bio-One GmbH, Germany.

2.2. Preparation of surfaces

All the biocompatible surface coatings were produced on standard microscope glass slides. Nanostructured nonpolymer-layered slides with hydrophilic surface and hydrophilic-superhydrophobic patterned surfaces were both purchased from Aquarray GmbH (Eggenstein-Leopoldshafen, Germany). Nanoporous HEMA-EDMA smooth surface was prepared as described previously [41,42]. Briefly, glass slides (75 × 25 mm) were coated with a 10- to 20-μm thick nanoporous poly(2-hydroxyethyl methacrylate-*co*-ethylene dimethacrylate (HEMA-EDMA) polymer layer, followed by esterification of the polymer layer with 4-pentynoic acid. Thereafter, the polymer was modified with

cysteamine hydrochloride using UV-induced click photopatterning to generate hydrophilic surface [41,42]. To prepare HEMA-EDMA rough surface with increased roughness and hydrophilicity, the superficial layer of HEMA-EDMA polymer coating was removed with adhesive film ("Scotch tape") [41,42]. Preparation of poly(thioether) dendrimer surface was done as described previously [43]. Briefly, the surface of a standard microscope glass slide was silanized using triethoxyvinylsilane followed by a repetitive reaction cycle consisting of a thiol-ene photoclick reaction using 1-thioglycerol and an esterification reaction using pentenoic acid. A dendrimer-modified surface of the third generation was finally functionalized in another thiol-ene reaction using 1-thioglycerol to create a hydrophilic surface.

2.3. Water contact angle measurement

The static water contact angles (WCAs) for different hydrophilic surfaces were measured as described previously [44]. Briefly, 5 μL deionized water was placed as a droplet on different surfaces, and static WCAs were measured by a Drop Shape Analyzer machine according to manufacture protocol (Krüss, Hamburg, Germany).

2.4. Cell culture

HeLa-CCL2 cells were cultured at 37 °C with 5% CO_2 in Dulbecco's modified eagle medium supplemented with 10% fetal bovine serum and 1% penicillin-streptomycin solution. Cells were tested and found free of any mycoplasma contamination.

2.5. Scanning electron microscopy

For scanning electron microscopy (SEM) of cultured HeLa-CCL2 cells, those were grown on different surfaces for 24 h until reaching confluency. After that, cells were washed with phosphate-buffered saline, and attached cells were fixed on the surface with 2.5% glutaraldehyde for 1 h. Next, cells were dehydrated in different concentrations of ethanol (30%, 50%, 75%, 85%, 95%, and 100%), with 10-min incubation in each. Cells were thereafter incubated in 1:1 solution of HMDS and ethanol for 30 min. Finally, cells were incubated in 100% HMDS for 30 min. Both empty hydrophilic surfaces (without cells) and surfaces with HeLa-CCL2 cells were sputter coated with platinum to a thickness of 5 nm before imaging on an LEO 1530 scanning electron microscope (Carl Zeiss Microscopy GmbH, Germany).

2.6. Atomic force microscopy

The surface topographies of all five surface coatings were investigated with a *Dimension Icon* with *ScanAsyst* from Bruker (Billerica, USA). Cantilevers with a resonance frequency of 325 kHz from Olympus (Shinjuku, Japan) were used. The scanned surface dimensions were 10 × 10 μm, and three different spots were examined for each surface. The R_a values were calculated for the full surface areas and produced as average, whereas average error was determined from the software *Gwyddion V. 2.56* (GPL). Depending on the surface roughness, the amplitude set point, the proportional gain, and the integral gain were adjusted. The scan rate was constant at 1 Hz.

2.7. Actin staining

HeLa-CCL2 cells were grown onto different hydrophilic surfaces for 24 h and fixed onto the surface using 4% paraformaldehyde for 1 h. Next, cells were washed using phosphate-buffered saline, and cell membranes were permeabilized with 0.1% Triton X-100 for 15 min. Cells were washed again and incubated with 1% bovine serum albumin for 1 h. Next, cells were incubated in appropriate concentration of Phalloidin-Atto 565 dye and Hoechst 33342 in phosphate-buffered saline for 1 h. Sections were air dried and mounted using aqueous mounting medium on thin glass slides. Sections were imaged using Leica TCS SPE confocal microscope (Leica Microsystems CMS GmbH, Germany) with 20× objective lens. Cellular area was determined using ImageJ software, National Institutes of Health (NIH) [45]. Unpaired two-tailed *t*-test was used to calculate any significant difference in the area of cells cultured on different surfaces, with respect to those grown in Petri dish.

2.8. Assessment of cell viability

HeLa-CCL2 cells were grown at appropriate densities for 24 h on hydrophilic spots of different sizes of nanostructured nonpolymer-layered droplet microarray. Next, cells were incubated for 15 min at 37 °C with 0.4 μg/mL of Calcein AM and 0.8 μg/mL of propidium iodide in phosphate-buffered saline. Cells were imaged using fluorescence microscope Keyence BZ-9000 (KEYENCE, Osaka, Japan) with 10× objective lens. Cellular viability was estimated by the percentage of Calcein AM–positive cells with respect to total number of cells. Significant differences in cellular viability at different volumes on DMA with respect to control were estimated using unpaired two-tailed *t*-test.

2.9. Cell seeding, RNA isolation, and next-generation sequencing

HeLa-CCL2 cells were grown onto glass slides layered with different biocompatible coatings (nanostructured nonpolymer, HEMA-EDMA smooth, HEMA-EDMA rough, and poly(thioether) dendrimer). Before cell seeding onto different substrates and nanoliter volumes, we first prepared a "humidity chamber" for the slides. For each surface, the lid of a sterile 100 mm cell culture Petri dish was layered with wetted tissues, and ~2 mL of sterile phosphate-buffered saline was added to the Petri dish. The "humidified Petri dish" was tested to maintain a constant humidity to prevent evaporation of the cell culture medium from the hydrophilic surfaces and also from the nanoliter cell culture reservoirs on DMA. The hydrophilic slides were sterilized with 70% ethanol, dried on air, and placed inside the aforementioned humidified Petri dish. Around 1.5–2 mL of cell suspension (~0.2 million cells/mL) was added onto the hydrophilic layer, and cells were cultured for 24 h inside a cell culture incubator. In Petri dish, cells were grown as usual for 24 h until 80% confluency. Cells from three hydrophilic slides were pooled together for RNA isolation using RNeasy Mini kit, according to manufacturer's protocol. HeLa-CCL2 cells were also cultured for 24 h in various nanoliter media volumes (100 nL, 9 nL, and 3 nL) on nanostructured nonpolymer-layered DMA containing hydrophilic spots with side lengths of 1 mm, 500 μm, and 350 μm, respectively. For this, "rolling droplet" method of cell seeding was used, as described previously [24]. Briefly, each patterned DMA slide was sterilized with 70% ethanol, dried, and placed inside the humidified Petri dish. The hydrophilic spots on each type of patterned DMA (1 mm, 500 μm, and 350 μm) were divided into three fields (Fig. 1), separated by superhydrophobic borders. Approximately 1.5 mL of cell suspension (with desired cell concentration/mL; Fig. 6a) was added onto each hydrophilic field on DMA and allowed for cells to be settled for 30 s. Then the DMA slide was slightly tilted causing the 1.5 mL droplet to roll off the slide, forming an array of separated nanoliter droplets at the hydrophilic spots. Next, the Petri dish containing patterned DMA slides with cells was incubated for 24 h inside the cell culture incubator. Cells from five DMA slides were pooled for each group, and mRNA was isolated as described earlier. Cells were seeded in 96-well plate in density of 10,000 cells/well and cultured for 24 h before mRNA isolation.

Both quality and quantity of total RNA samples were assessed with a Bioanalyzer (Agilent Technologies GmbH, Germany) and RNA chip. Libraries were prepared from 1 μg of total RNA with the Illumina TruSeq stranded mRNA Kit, following manufacturer's recommendations. Quality and quantity of libraries were assessed with Bioanalyzer on high-sensitivity DNA chip. Libraries were sequenced as paired-end (2 × 100 nucleotides) reads on a HiSeq4000 (Illumina GmbH, Germany). Raw sequencing data were demultiplexed with Illumina Bcl2fastq tool, and the quality was assessed with the FASTX tool kit [46]. Reads were

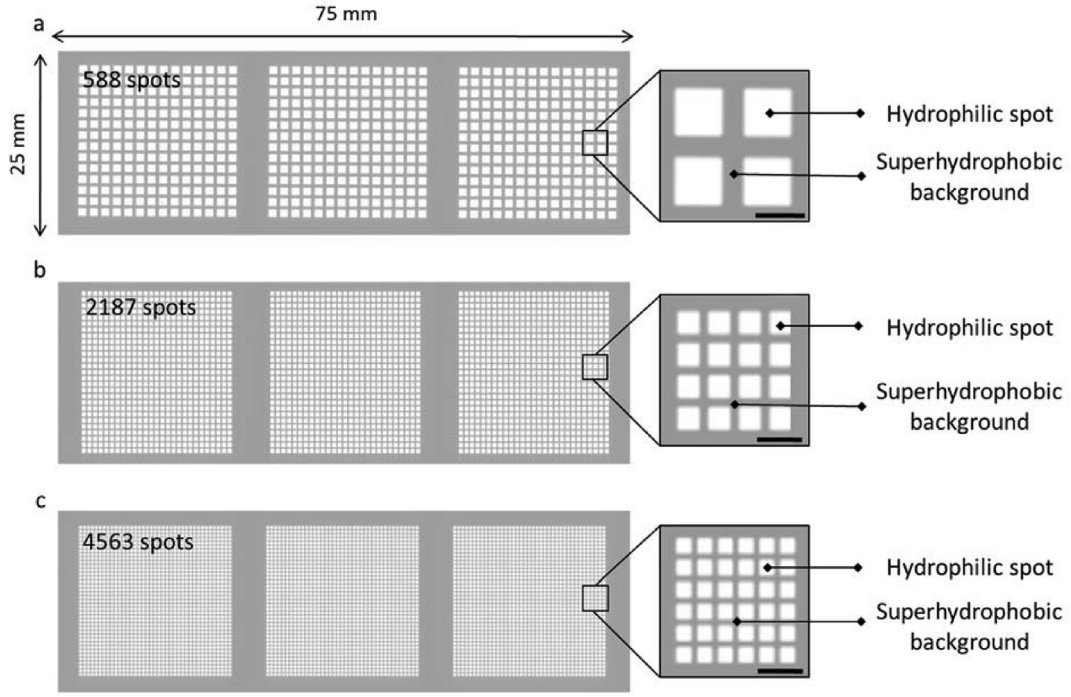

Fig. 1. Droplet microarray (DMA) platform. Schematic representation of DMA sides with hydrophilic square spots having side lengths of (a) 1 mm, (b) 500 μm, and (c) 350 μm. Scale bar = 1 mm.

mapped against the human reference genome GRCh38 with STAR alignment tool using default parameters [47]. Raw counts were computed at gene level with HTSeq tool in union mode [48]. Gene expression was normalized with DESeq2 [49]. A log base 2 of the fold change (log2FC) was computed for pairwise comparison of samples. Differentially expressed genes (DEGs) were identified with $\leq +2$ or ≥ -2 log2 fold change of expression. Enriched gene ontology (GO) terms associated with DEGs were tested with the one-tailed exact Fisher test corrected by false discovery rate (FDR) /multiple testing methods [50]. Samples or genes were clustered with hierarchical methods applied on Euclidean distances.

3. Results and discussion

3.1. Characterization of the surfaces for fabrication of DMA

DMA is a versatile tool for miniaturized high-throughput screenings of live cells. Fig. 1 shows schematic representation of Droplet microarrays containing 588, 2187, and 4563 square hydrophilic spots with side length of 1 mm, 500 μm, and 350 μm, respectively, which we have used in this study.

Our goal was to investigate the differential molecular response of HeLa-CCL2 cells cultured onto traditional cell culture platform versus different surface coatings used to fabricate DMA. For our study, we have selected the following four surfaces commonly used for fabrication of hydrophilic-superhydrophobic DMA: (1) nanostructured nonpolymer, (2) rough and (3) smooth variants of HEMA-EDMA polymer, and (4) poly(thioether) dendrimer. All these surfaces were chosen because of their biocompatibility (compatibility with cell culture), possibility for chemical modification (compatibility with hydrophilic-superhydrophobic patterning), and transparency (compatibility with microscopy). On the other hand, these four surface coatings are distinctly different to each other in terms of chemical composition, wettability, and surface roughness (Fig. 2 and Fig. S1, respectively). As cellular response has been shown to be greatly influenced by both surface topography and chemical properties [32–34], these four surface coatings of unique biocompatible features were particularly selected for testing the molecular response of HeLa-CCL2 cells cultured on them. Standard cell culture Petri dish is a traditional, "state-of-the-art" platform for regular cell culture in laboratories, so it was used as the suited control for our study.

We analyzed wettability of the surfaces using static WCA measurement, whereas topographies of hydrophilic surfaces were investigated with atomic force microscopy (AFM) and SEM, with cell culture Petri dish as the reference. Fig. 2a–e provides the schematic representation of all the surfaces investigated in this study. On measuring static WCA of the hydrophilic surfaces under investigation, HEMA-EDMA rough surface was found to be the most hydrophilic (static WCA 9 ± 1°), whereas conventional cell culture Petri dish demonstrated the least hydrophilicity (static WCA 52 ± 1°; Fig. 2f–j). Advancing and receding WCAs on the hydrophilic surfaces could not be measured because of the very low values. Other surfaces, that is, nanostructured nonpolymer, HEMA-EDMA smooth, and poly(thioether) dendrimer had static WCAs as 21 ± 1°, 22 ± 1°, and 33 ± 1°, respectively (Fig. 2f–j). Via AFM measurement, we have demonstrated that investigated surfaces had different surface topographies (Fig. S1). HEMA-EDMA rough surface was created by removing the top polymer layer, as described in detail in the experimental section. In terms of the mean surface roughness (Ra), HEMA-EDMA rough surface coating was found to have the maximum Ra value (70.7 ± 2.3 nm), whereas poly(thioether) dendrimer had the least Ra (0.2 ± 0.02 nm) among all the investigated surfaces (Fig. S1). Ra values from nanostructured nonpolymer, HEMA-EDMA smooth, and conventional cell culture Petri dish were found to be 48.0 ± 1.7 nm, 18.1 ± 0.4 nm, and 2.9 ± 0.2 nm, respectively (Fig. S1). SEM images of the surfaces further confirmed the distinctiveness of all the five surfaces in terms of porosity and roughness (Fig. 2k–o). We further wanted to assess any potential effect of the different surface coatings on cellular morphology. SEM images of HeLa-CCL2 cells grown on the investigated surface coatings and on Petri dish as the control are shown in Fig. 2p–t. Our results indicate that the cells cultured on different surfaces do not exhibit any visual difference, as cells on all surfaces were found to be flattened and demonstrated the usual morphology of HeLa-CCL2 cells (Fig. 2p–t). Henceforth, all the investigated surface coatings revealed biocompatibility but demonstrated different surface properties with topography/

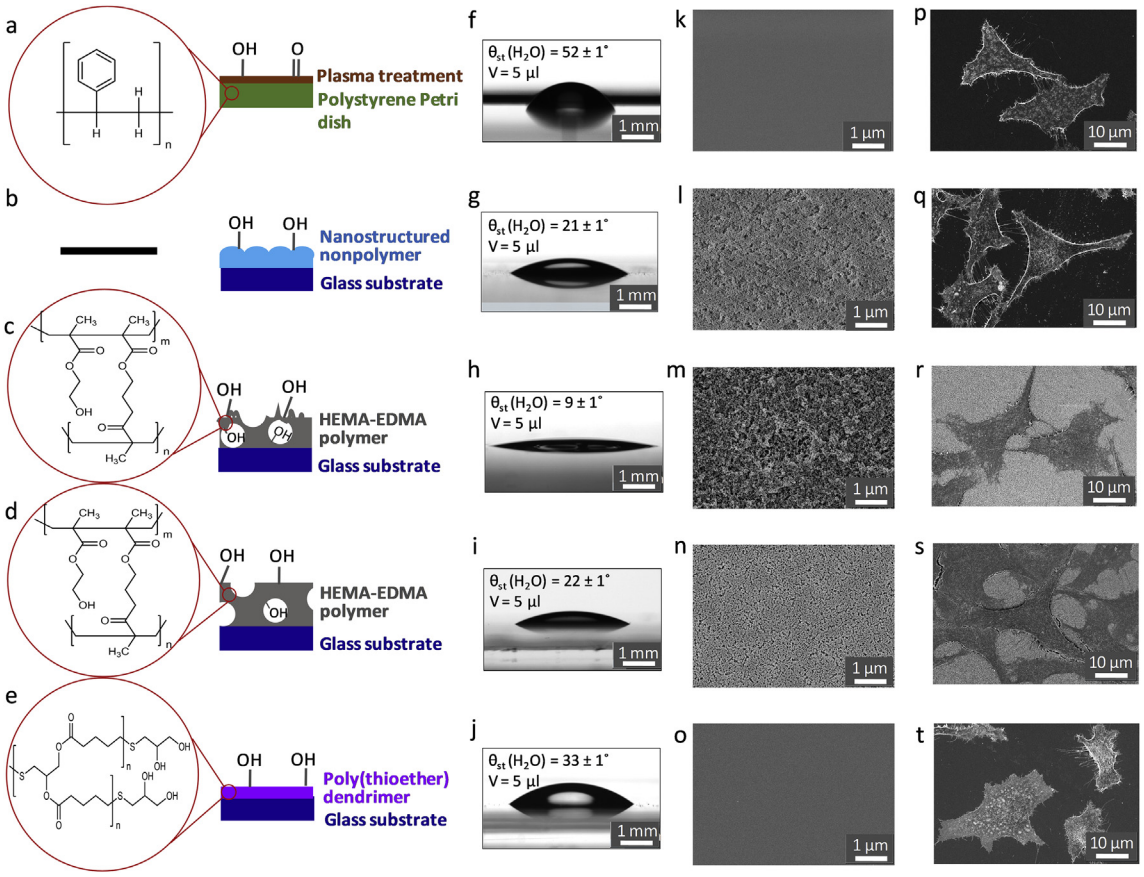

Fig. 2. Schematic representation, water contact angles, and scanning electron microscopy images of hydrophilic surfaces (without and with HeLa-CCL2 cells) under investigation. (a–e) Schematic representation of mentioned surfaces. (f–j) Water contact angles ± SD from four independent measurements. Scale bar = 1 mm (k–o). Scanning electron microscopy (SEM) of empty hydrophilic surfaces. Scale bar = 1 µm. (p–t) SEM for HeLa-CCL2 cells cultured on different hydrophilic surface coatings. Scale bar = 10 µm. The sequence of the surfaces under investigation are Petri dish (f, k, p), nanostructured nonpolymer (g, l, q), HEMA-EDMA polymer rough (h, m, r), HEMA-EDMA polymer smooth (i, n, s), and poly(thioether) dendrimer (j, o ,t), respectively.

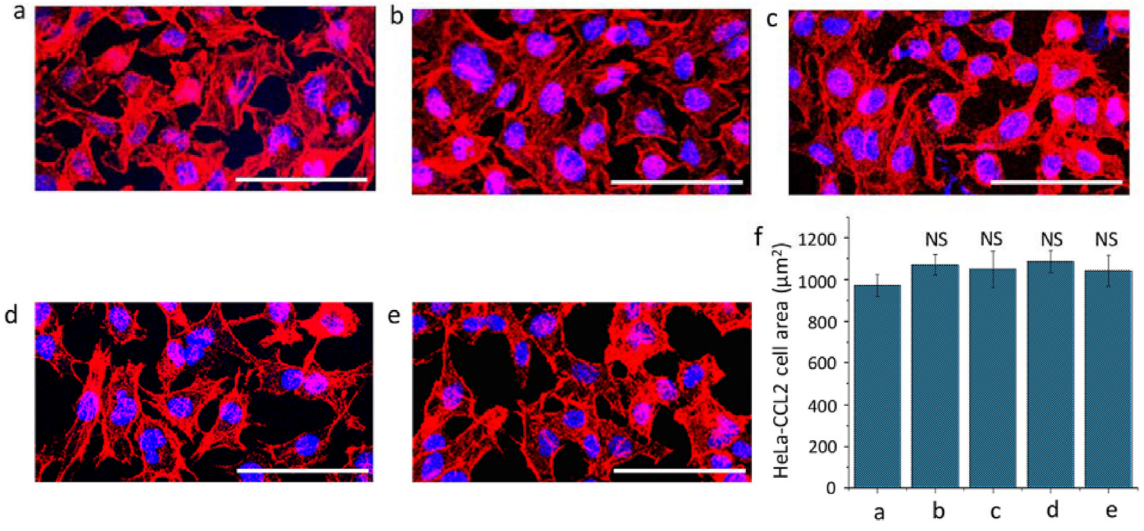

Fig. 3. Peripheral actin staining of HeLa-CCL2 cells cultured on different surface coatings. Confocal microscopy images of HeLa-CCL2 cells grown for 24 h on (a) Petri dish, (b) nanostructured nonpolymer, (c) HEMA-EDMA polymer rough, (d) HEMA-EDMA polymer smooth, and (e) poly(thioether) dendrimer surface. Actin and nuclei were stained by Phalloidin-Atto dye and Hoechst 33342 stain, respectively. Scale bar = 100 µm. (f) Graph showing area of HeLa-CCL2 cells grown on different surfaces, as marked by actin staining. Data represented as mean ± SEM, n = 20 cells analyzed per surface. Any significant difference in the area of HeLa-CCL2 cells grown on different surfaces with respect to those cultured on Petri dish was calculated by two-tailed unpaired *t*-test. NS = not significant.

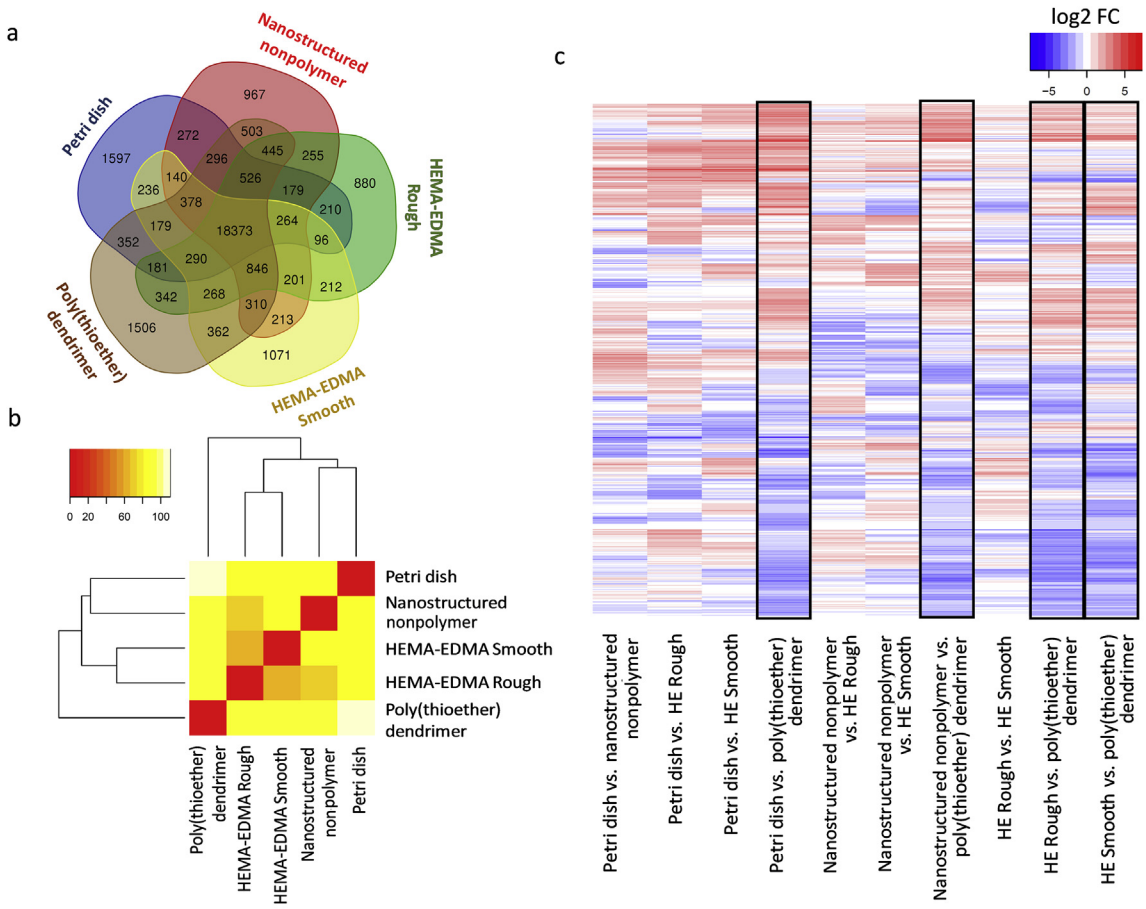

Fig. 4. Comparative transcriptome analysis of HeLa-CCL2 cells grown on different biocompatible surface coatings. (a) Venn diagram showing the distribution of all genes expressed in HeLa-CCL2 cells cultured on different surfaces. (b) Cluster analysis of transcriptome of HeLa-CCL2 grown on different surfaces. Hierarchical clustering was done based on Euclidean distance. (c) Pairwise comparison of DEGs between different surfaces. Color gradient is determined by log2 fold change of expression (log2 FC).

surface roughness ranging from smooth (0.2 nm) to rough (70.7 nm) and static WCAs reflecting hydrophilicity ranging from 9° to 52°.

3.2. Effect of different surface coatings on the morphology of HeLa-CCL2 cells

As the next step, we have further investigated the effects of all the four surfaces on cell morphology by staining the cytoskeletal actin of HeLa-CCL2 cells. The distribution of cellular actin is important for identification of any differences in the cell size, cytoskeleton, and morphology upon culturing on substrates with different topography and roughness. HeLa-CCL2 cells were cultured for 24 h on different substrates, and confocal microscopy was done to analyze the cellular area based on peripheral actin staining (Fig. 3a–e). Cells demonstrated the usual morphology, which is also an indirect measure for cell viability because viable HeLa-CCL2 cells are adherent by nature, whereas dead cells usually lose their surface adhesive properties. No significant difference in the cellular area was observed among different substrates (Fig. 3f). Taking together, HeLa-CCL2 cells grown on all four surfaces did not show any apparent difference in morphology and viability.

3.3. Effect of different surface coatings on transcriptomic landscape of HeLa-CCL2 cells

To get a broader overview of the cellular behavior after being cultured on different substrates, we aimed to analyze the transcriptome of HeLa-CCL2 cells grown on all surfaces under investigation for 24 h. Unlike the proteome, transcriptomic alterations can be well observed as early as after 24 h of cell culture [51,52]. Therefore, we have chosen to culture HeLa-CCL2 cells for 24 h, although cells on DMA can be cultured for up to 3–7 days depending on the culturing conditions [24,30]. In this study, cells were cultured on different substrates for 24 h followed by RNA isolation and mRNA sequencing. For all the samples, more than 90% of the reads had a Phred score (Q) greater than 30, and more than 50 million reads were mapped to the human reference genome GRCh38 (Table S1). Nearly 78% of the genes expressed in the cells grown on Petri dish were also expressed consecutively among the other surfaces (Fig. 4a). The surfaces were grouped according to global variation in gene expression with the hierarchical clustering method (Fig. 4b). Our results yielded few interesting observations: (1) transcriptome of cells cultured on nanostructured nonpolymer surface had the closest resemblance to that of cells cultured on Petri dishes, despite the differences in these two surfaces in terms of porosity and roughness (Fig. S1); (2) HeLa-CCL2 transcriptome data from HEMA-EDMA smooth and rough surfaces were clustered together, probably as these two substrates share the same polymer chemical composition, albeit with different topographical features; (3) cells grown on poly(thioether) dendrimer surface exhibited the most diverse transcriptomic pattern from cells cultured on Petri dish, although both poly(thioether) dendrimer substrate and Petri dish have smooth surfaces, as observed by AFM and SEM (Fig. S1 and Fig. 2, respectively). From these three observations, we can conclude that surface porosity and roughness alone are not the most critical factors in determining cellular gene expression in the case of the investigated surfaces. In our study, the cellular transcriptome is likely influenced by

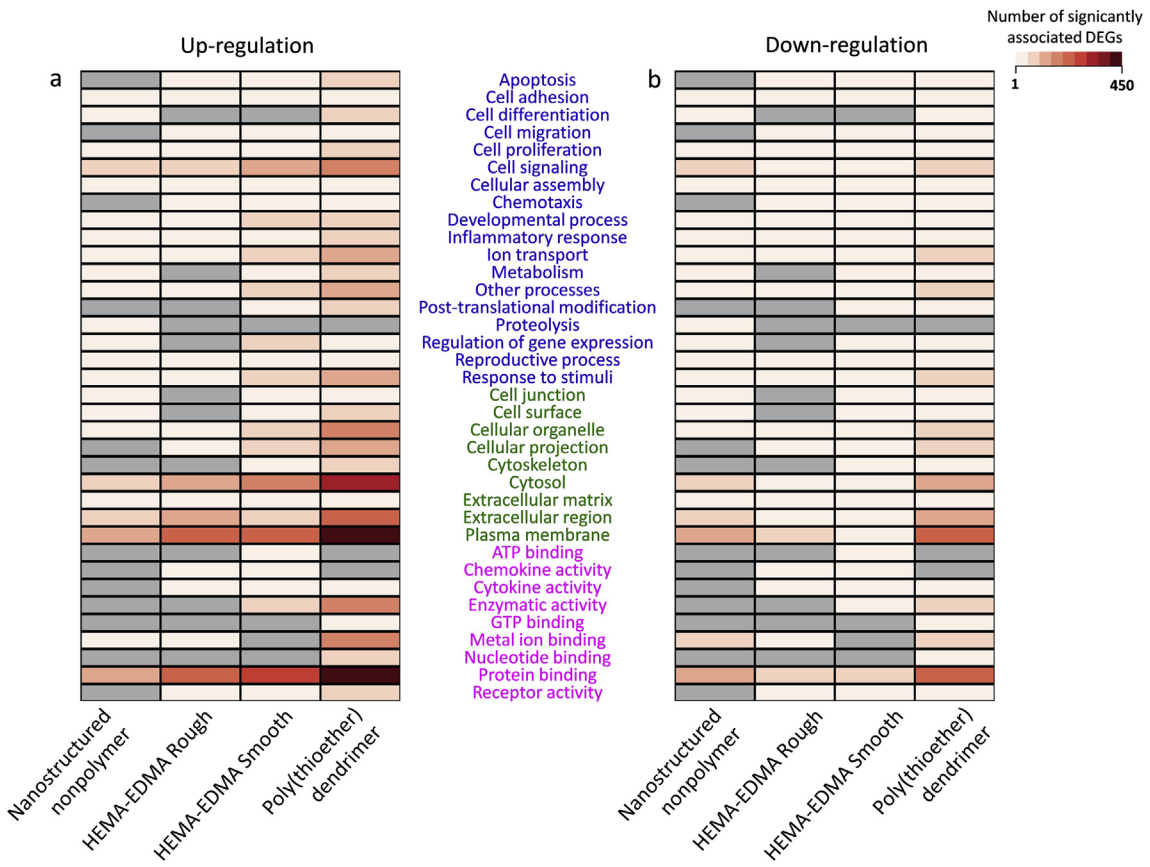

Fig. 5. Gene ontology analysis for differentially expressed genes in HeLa-CCL2 cells cultured on different surface coatings. Number of DEGs associated with GO terms in (a) upregulation and (b) downregulation category. Gray color in the heatmap represents no significant enrichment with the respective GO term. DEGs belonging to biological process, cellular component, and molecular function were grouped and highlighted in blue, green, and magenta color, respectively.

combinatorial factors that could encompass a proper balance between topography and wettability of the cell culture surface. To our knowledge, this is the first study analyzing the cellular transcriptome post culture on HEMA-EDMA polymer and our in-house nanostructured nonpolymer surfaces. In the literature, it has been shown that both topography and chemistry of a surface can influence the biology of cells [32–34]. However, this phenomenon is highly dependent on the particular surface and type of cells under investigation, so the results are expected to vary with different substrates and cell lines.

Comparison of gene expression levels in cells cultured onto each investigated surface and in Petri dish demonstrated that only a minority of genes were differentially expressed. The percentage of DEGs among all expressed genes was less than 5% for nanostructured nonpolymer, HEMA-EDMA rough and HEMA-EDMA smooth, but 9.45% for poly(-thioether) dendrimer substrate (Table S2). This pattern for the distribution of DEGs across surfaces was also represented in a heatmap (Fig. S2). Among the DEGs, 138 were common between all the surfaces (Fig. S3). We further compared the DEGs among each surface pairs. As shown in the heatmap, cells cultured on poly(thioether) dendrimer surface was found to harbor the highest number of DEGs in comparison to that of other surfaces and Petri dish, confirming the greatest (from all four surfaces) influence of dendrimer surface on cellular transcriptome (Fig. 4c).

3.4. GO analysis of DEGs from HeLa-CCL2 cells cultured on different surfaces

To explore the biological functions of DEGs across the investigated surfaces, GO enrichment analysis was carried out. All four surfaces had similar trend of having less number of downregulated DEGs with GO terms than the upregulated ones. We did not observe any distinct transcriptomic indication of compromised cell survival in any of the four biocompatible surfaces, compared with the HeLa-CCL2 transcriptome data from Petri dish (Fig. 5a and b). We could observe that a major share of DEGs across all surfaces were comprised of genes related to certain cellular components and protein binding (Fig. 5a and b). This is not surprising, as expression of genes regulating cellular components and binding affinities are often influenced by cell-biomaterial interactions [53]. As indicated from the earlier heatmaps as well (Fig. S2 and Fig. 4c), HeLa-CCL2 cells grown in poly(thioether) dendrimer surfaces harbored the highest number of DEGs implicated in several biological processes, with most of the upregulated genes associated with plasma membrane and protein binding functions (Fig. 5a). We had a closer look at the upregulated DEGs in HeLa-CCL2 cells cultured on poly(thioether) dendrimer surface and found a number of genes related to membrane-associated functions, that is, cell surface and microtubule-associated proteins, such as *ITGB3* and *KIF21B* [54,55]. Upregulation of these cell surface protein-coding genes indicates that cells might have to adapt themselves in order to adhere to this surface. Furthermore, upregulation in certain cell surface transporter-coding genes such as *SLC38A3* and *SLC26A9* indicates enhanced amino acid and ionic transport in HeLa-CCL2 cells cultured on this surface [56,57]. These cell surface related changes might have in turn led to alterations in protein binding and cell signaling pathways, as reflected by increased expression of transcription factor-coding genes such as *TRAF1* and *SDC4* [58,59]. Dendrimers are an excellent tool for a wide range of biomedical applications, including nonviral siRNA delivery or drug delivery to cultured cells [60,61]. Polypropylenimine dendrimers are reported to have regulatory effects on endogenous gene expression in a strong cell-type dependent manner [62], whereas carbosilane dendrimers

a

Cell culture platform	Cell culture area (mm^2)	No. of hydrophilic spot or well	Culture volume	Cell conc. for seeding (Million/mL)	No. of cells in each spot or well	Cell culture area/ cell numbers (mm^2)	Culture volume/cell numbers (nL)	Total no. of cells
96 well	34	1	100 μL	0.1	10000	0.003	10	960000
1 mm	1	588	100 nL	1	100	0.01	1	58800
500 μm	0.25	2187	9 nL	2.8	25	0.01	0.36	54675
350 μm	0.12	4563	3 nL	4.3	12	0.01	0.25	54756

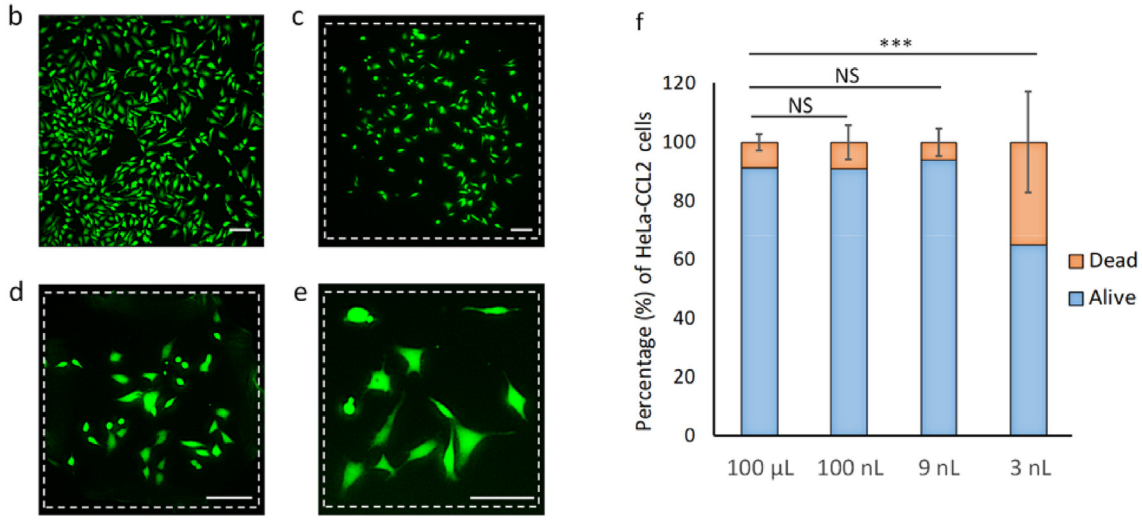

Fig. 6. HeLa-CCL2 cell culture on nanostructured nonpolymer-layered DMAs with various sizes of hydrophilic spots. (a) Total number of cells in 96-well plate and 1 mm, 500 μm, and 350 μm hydrophilic spots on a DMA slide. (b–e) Fluorescence microscopy images of Calcein AM staining in HeLa-CCL2 cells grown for 24 h in 96-well plate and on 1 mm, 500 μm, and 350 μm hydrophilic spots, respectively. Scale bar = 100 μm. (f) HeLa-CCL2 cellular viability analysis post 24 h of culture in 100 μL media (96-well plate) and different culture volumes on DMA (100 nL, 9 nL, and 3 nL). Percentage of live (Calcein AM–positive) cells were calculated with respect to the total number of cells (sum of Calcein AM–positive and propidium iodide–positive cells). Data from 10 wells were analyzed for 96-well plate. At least 30 hydrophilic spots were analyzed for each hydrophilic spot size on DMA. Data represented as mean ± SEM.***$P < 0.001$ according to two-tailed unpaired *t*-test, calculated as differences in cellular viability in different nanoliter volumes on DMA with respect to control (100 μL in 96-well plate). NS = not significant.

(2G-NN16) are found to alter gene expression for immune response, transcriptional regulation, and cell proliferation in macrophages [63]. As evidenced from the GO analysis of DEGs (Fig. 5a and b) as well as phenotypic observations (Fig. 3e and f) of HeLa-CCL2 cells on poly(-thioether) dendrimer, we find this surface compatible with cellular assays. The unique transcriptomic influence of different dendrimeric surfaces on cells is likely dependent on the surface topography and chemistry of the dendrimer surface, as well as the cell type under exploration.

Our results indicate that all the four substrates used here for cell culture had minimal effects on transcriptomic alternations in HeLa-CCL2 cells in comparison to the traditional Petri dish. The major share of upregulated genes from all the surfaces were from the membrane-associated or protein binding category, indicating the cellular adaptation to bind to different substrates. Our findings therefore suggest that the cells cultured on alternative substrates can exhibit comparable properties to cells grown on commonly used platforms, indicating the possibility of using such novel surfaces for routine cell culture experiments along with commonly used Petri dishes and microtiter plates.

3.5. *HeLa-CCL2 cell culture in different nanoliter media volumes on nanostructured nonpolymer-layered patterned DMA*

With a growing demand for higher throughput and miniaturization of cell culture vessels, culturing cells in picoliter to nanoliter volumes becomes essential. DMA platform enables high-throughput cell screenings in nanoliter droplets. However, the effect of small cell culture volumes on the underlying cell biology needs to be explored and compared with cells cultured in conventional cell screening platforms. Ninety six-well plates are popularly used for cell screening experiments in biological research and have the similar surface architecture as Petri dish. Here we have compared the biological state of HeLa-CCL2 cells cultured in nanoliter volumes on DMA, with that of the same in 96-well plate. Viability and morphology of HeLa-CCL2 cells were investigated upon culturing on DMA with square hydrophilic spots having side lengths of 1 mm, 500 μm, and 350 μm. We have used discontinuous dewetting for seeding the cells on the DMA. In this case, the volume of cell culture media is determined by the size of the hydrophilic spots. The culture volume retained within these three sizes of hydrophilic spots are 100 nL, 9 nL, and 3 nL respectively, as determined previously by the measurement of droplet height and weighing a certain number of formed droplets on each type of DMA [24]. DMAs for this experiment were fabricated onto nanostructured nonpolymer-layered substrates because cells cultured onto this surface were found to have the closest transcriptomic resemblance to those grown on the Petri dish. In all the DMA slides, cells were seeded using the “rolling droplet” method without the need for any robotics or pipetting, as described in the “Materials and Methods” section.

The ratio of volume-to-cell and area-to-cell is different in 96-well plate and on different types of DMA. In 96-well plate, there is 10 nL of cell culture media per single cell, whereas on DMA, there is 1 nL, 0.36 nL, and 0.25 nL of cell culture media per single cell for 1 mm, 500 μm, and 350 μm hydrophilic spots, respectively (Fig. 6a). The cell culture area is 0.003 mm^2 per single cell in 96-well plate, whereas it has been kept constant at 0.01 mm^2 per single cell on DMA (Fig. 6a). The reduced culture media volume per cell on DMA is expected, as it is an established platform for effective miniaturization of regular cell culture and cell screening

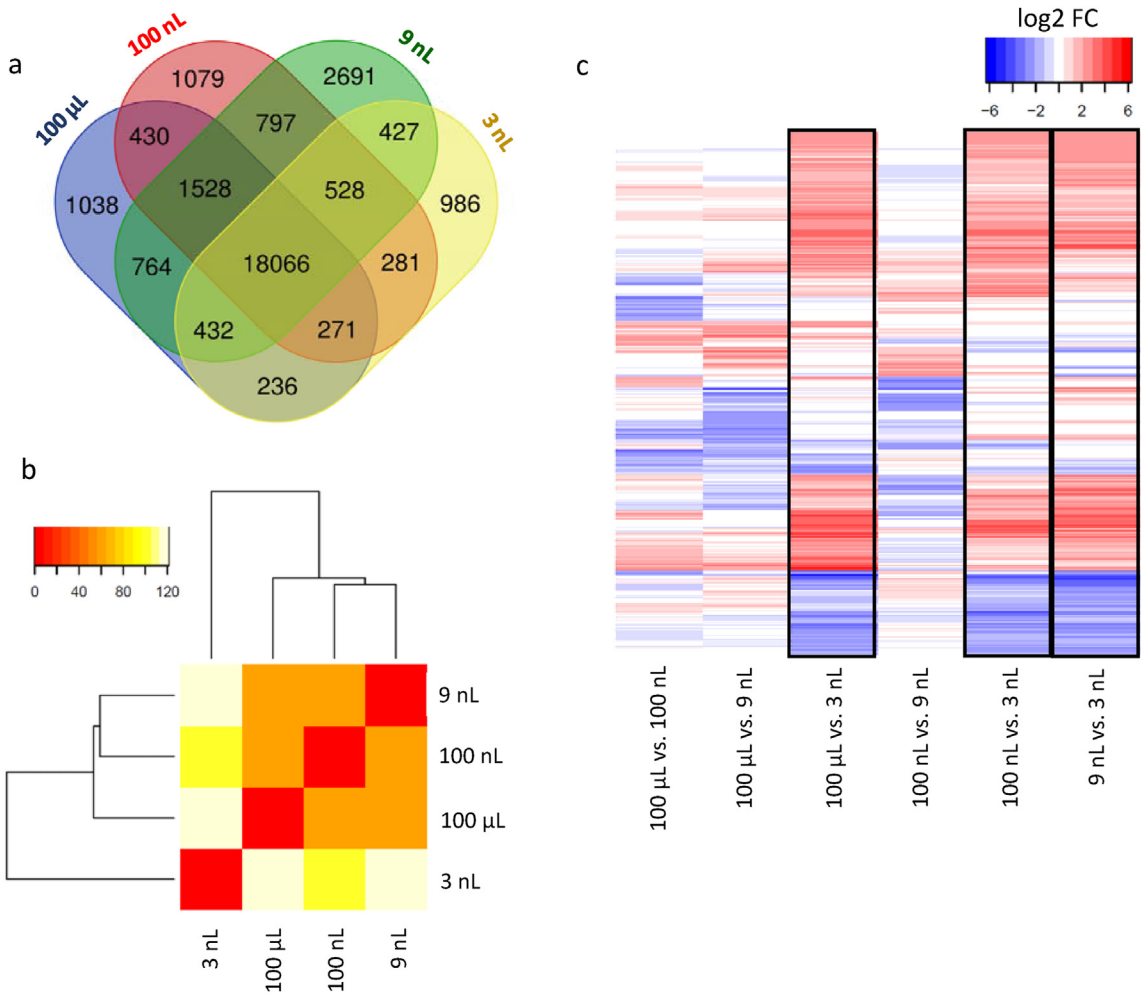

Fig. 7. Comparative transcriptome analysis of HeLa-CCL2 cells grown on DMA in various nanoliter culture media volumes. (a) Venn diagram showing distribution of all genes expressed in HeLa-CCL2 cells cultured in different culture media volumes on DMA. Cells cultured in 96-well plate in 100 µL were taken as a control. (b) Cluster analysis of HeLa-CCL2 transcriptome from different culture volumes. Hierarchical clustering was done based on Euclidean distance. (c) Pairwise comparison of DEGs between different sampling groups. Color gradient is determined by log2 fold change of expression (log2 FC).

experiments. The goal of performing transcriptomic studies in different volumes on DMA was precisely to investigate if this reduction of volume-to-cell ratio and increase of area-to-cell ratio has any direct or indirect influence on the molecular response of cells.

To check cellular viability 24 h post seeding, cells were stained with Calcein AM and propidium iodide. Fig. 6b–e shows the viable (Calcein AM stained) HeLa-CCL2 cells in hydrophilic spots of different sizes on DMA and 96-well plate, 24 h post seeding. Viability of cells was found above 90% in 100 nL and 9 nL cell culture droplets, comparable to that in 96-well plate (100 µL). However, HeLa-CCL2 cells had approximately 65% viability in 3 nL culture volume. The reason for this compromised viability in this culture volume could be multifactorial, that is, (1) limited availability of nutrients, (2) quick acidification of the media because of higher concentration of cellular waste, or (3) relatively larger droplet volume fluctuation because of evaporation–condensation. Overall, our results indicate that viability of cells cultured for 24 h in droplets as small as 9 nL on an open DMA platform is comparable with the viability of cells grown in 100 µL volume in a 96-well plate.

3.6. Analysis of HeLa-CCL2 transcriptome post culture in different nanoliter cell media volumes on DMA

To gain a deeper understanding of possible effects of nanoliter volumes on cell culture, we analyzed the transcriptomic landscape of cells cultured on DMA. HeLa-CCL2 cells were cultured for 24 h in 100 nL, 9 nL, and 3 nL droplets on nanostructured nonpolymer-layered DMA and in 96-well plate (100 µL), followed by RNA isolation and mRNA sequencing. Quality information of sequenced data is provided in Table S3. A substantial number of transcripts (n = 18,066) were commonly expressed in all the samples (Fig. 7a). Cluster analysis indicated a close resemblance of cellular gene expression pattern with those cultured in 100 µL media volume in a 96-well plate and cells cultured in 100 nL or 9 nL cell culture media onto hydrophilic spots on DMA (Fig. 7b). Cells cultured in 3 nL culture media on 350 µm hydrophilic spots were clustered separately (Fig. 7b) and exhibited highest percentage of DEGs (Table S4), represented also as a heatmap (Fig. S4). We further performed pairwise comparison of DEGs from different nanoreservoirs and found that cells grown in 3 nL droplets possessed the most unique transcriptomic signature among all tested volumes (Fig. 7c). On comparison of DEGs expressed in all four media volumes, we found 80 DEGs that are commonly shared between groups (Fig. S5). Cells grown in 3 nL media displayed the highest number of DEGs in comparison to control and cells grown in other hydrophilic spot sizes. The unique transcriptomic pattern of cells grown in 3 nL droplets could be explained by possible cellular stress, as demonstrated by the lower cell viability compared with other culturing volumes, whereas the gene expression pattern of cells

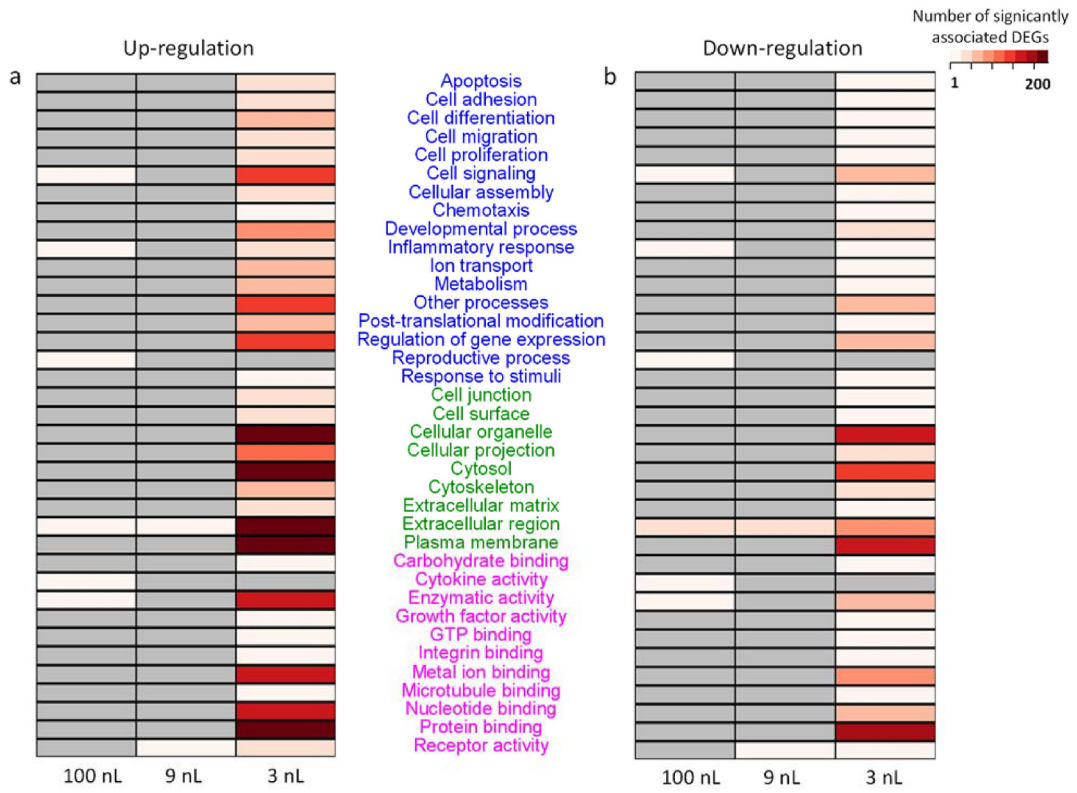

Fig. 8. Gene ontology analysis for differentially expressed genes from HeLa-CCL2 cells grown in different nanoliter culture volumes on DMA. The number of DEGs associated with GO terms both in (a) upregulation and (b) downregulation category. Gray color in the heatmap represents no significant enrichment with the respective GO term. DEGs belonging to biological process, cellular component, and molecular function were grouped and highlighted in blue, green, and magenta color, respectively.

cultured in 9 and 100 nL droplets closely resembled that of the cells cultured in 100 μL media volume within a 96-well plate.

3.7. GO analysis of DEGs from HeLa-CCL2 cells grown in different cell culture volumes on DMA

Next, we have performed GO analysis with the DEGs from cells grown in different volumes on DMA. Upon GO analysis, HeLa-CCL2 cells grown in 9 and 100 nL droplets were not found to have any drastic alternation in the cellular pathways compared with cells cultured in 100 μL. Most of the up- and down-regulated genes associated with GO terms were represented by cells cultured in the least culture media volume (3 nL) on 350 μm cell culture nanoreservoirs (Fig. 8a and b, respectively). Up- and down-regulated DEGs with GO terms represented by cells cultured in 3 nL medium were in diverse categories belonging to cellular organelle, cytoplasm, extracellular region, plasma membrane, and protein binding (Fig. 8a and b). The number of upregulated DEGs with associated GO terms was relatively higher than downregulated DEGs. A detailed look at the upregulated DEGs in cells grown on 3 nL droplets revealed the presence of genes such as *ASIC3* and *CCL8*, which is indicative of acidity-mediated hypoxic cellular microenvironment [64,65]. This is in congruence with our hypothesis of quick acidification of cell culture medium in 3 nL droplets because of the rapid accumulation of cellular metabolic waste. Moreover, the presence of genes such as *DTX1* among the upregulated DEGs point toward a hypoxia-mediated apoptotic cell death in 3 nL droplets on DMA [66], along with alterations in a large number of other genes in multiple pathways. The transcriptomic output is supported by a compromised cell survival (65%; Fig. 6f), indicating that this culture volume might not be optimal for culturing cells on an open DMA platform.

However, our results demonstrate that HeLa-CCL2 cells cultured in 100 nL and 9 nL droplets on DMA exhibited comparable gene expression profile to cells cultured with 96-well plates in 100 μL media volume.

4. Conclusion

In vitro cell culture is an important tool to decipher molecular mechanisms behind basic cellular processes. Polystyrene Petri dishes and microtiter plates are routinely used for cell culture and high-throughput experiments. However, these are also nonphysiological surfaces that can be used only as one of the model cell culture platforms available, and not as the only reference. Hence, it is important to fabricate and investigate novel platforms with different properties to provide a cell culture environment that is closer to the physiological milieu. The four biocompatible surface coatings used in the present study are distinctly different to each other in terms of hydrophilicity, surface topography, and roughness, as indicated by the results from WCA measurement, SEM, and AFM, respectively. Here, we assessed the biocompatibility of these different surface coatings and nanoliter culturing reservoirs on DMA platform by comparing the phenotype and global transcriptome analysis of HeLa-CCL2 cells cultured on them, with that of conventional cell culture Petri dish and 96-well plates. HeLa-CCL2 cells cultured on the four different substrates exhibited comparable morphology and viability with those cultured in a conventional Petri dish. Differential transcriptome analysis demonstrated no drastic transcriptomic alterations in cells cultured on investigated surfaces compared with cells grown in the "state-of-the-art" platform. Transcriptome of cells grown on nanostructured nonpolymer coatings exhibited the closest resemblance to standard cell culture Petri dish, whereas cells cultured on poly(thioether) dendrimer surface had the highest number of DEGs. This finding indicates that in case of the investigated surfaces, combinatorial factors guiding a balance between topography and wettability played the

determining role in influencing cellular transcriptome. Morphology, viability, and gene expression pattern of cells cultured in 100 and 9 nL droplets on DMA were also found comparable with cells grown in 96-well plates that are cultured in upto four orders of magnitude higher volumes of 100 μL. This indicates that cells can be cultured in droplets as small as 9 nL on an open DMA platform in a standard cell culture incubator under controlled humidity without any oil to prevent evaporation, at least for 24 h, inducing no change in their biological properties. Future investigations on the alternations in different biological processes, that is, cellular metabolism, differentiation, inflammatory response etc. after long-term culture of cells on different surfaces and in restricted culture volumes could be interesting. Our findings from the present study shall contribute to an understanding and a paradigm shift in a broad scientific community, indicating that the same screening experiments that are performed in microtiter plates in microliter volumes can be performed on alternative surfaces with chemically and physically defined properties in nanoliter (three order of magnitude smaller) volumes.

Authors' contributions

S.C. contributed to conceptualization, investigation, visualization, and writing the original article. V.G. contributed to formal analysis, investigation, and visualization. M.B. contributed to resources. J.M.S. contributed to investigation. P.A.L. contributed to supervision and funding acquisition. A.A.P. contributed to conceptualization, supervision, and funding acquisition.

Data availability

The raw/processed data required to reproduce these findings cannot be shared at this time as the data also forms part of an ongoing study.

Declaration of competing interest

The authors declare the following financial interests/personal relationships which may be considered as potential competing interests: S.C., V.G., M.B., and J.S. declare no competing financial interests or personal relationships that could have appeared to influence the work reported in this article. A.P. and P.L. in addition to being employed by the KIT are also shareholders of Aquarray GmbH.

Acknowledgments

This research was supported by the Deutsche Forschungsgemeinschaft grant (DFG PO1820/3-1) and the Helmholtz Association's Initiative & Networking Fund (grant No. VH-NG-621). J.S. thanks Deutsche Bundesstiftung Umwelt for financial support. The authors sincerely thank Prof. Dr. Uwe Strähle for the next generation sequencing facility at the Institute of Biological and Chemical Systems–Biological Information Processing (IBCS–BIP), Karlsruhe Institute of Technology (Campus North). The authors are also thankful to Mr. Volker Zibat and the Laboratory for Electron Microscopy at Karlsruhe Institute of Technology (Campus South).

Appendix A. Supplementary data

Supplementary data to this article can be found online at https://doi.org/10.1016/j.mtbio.2021.100112.

References

[1] W.R. Earle, Production of malignancy *in vitro*. IV. The mouse fibroblast cultures and changes seen in the living cells, J. Natl. Canc. Inst. 4 (1943) 165–212.
[2] A.N. Brooks, S. Turkarslan, K.D. Beer, F. Yin Lo, N.S. Baliga, Adaptation of cells to new environments, Wiley Interdiscip. Rev. Syst. Biol. Med. 3 (2011) 544–561.
[3] T.G. Evans, Considerations for the use of transcriptomics in identifying the "genes that matter" for environmental adaptation, J. Exp. Biol. 218 (2015) 1925–1935.
[4] W. Zheng, N. Thorne, J.C. McKew, Phenotypic screens as a renewed approach for drug discovery, Drug Discov. Today 18 (2013) 1067–1073.
[5] E. Michelini, L. Cevenini, L. Mezzanotte, et al., Cell-based assays: fuelling drug discovery, Anal. Bioanal. Chem. 398 (2010) 227–238.
[6] D. Swinney, J. Anthony, How were new medicines discovered? Nat. Rev. Drug Discov. 10 (2011) 507–519.
[7] R.J. Petri, "Eine kleine Modification des Koch'schen Plattenverfahrens" (A small modification of Koch's plate method), Centralblatt für Bakteriologie und Parasitenkunde 1 (1887) 279–280.
[8] S. Barker, P. LaRocca, Method of production and control of a commercial tissue culture surface, J. Tissue Cult. Methods 16 (1994) 151–153.
[9] L. Ponsonnet, K. Reybier, N. Jaffrezic, V. Comte, C. Lagneau, M. Lissac, et al., Relationship between surface properties (roughness, wettability) of titanium and titanium alloys and cell behaviour, Mater. Sci. Eng. C 23 (2003) 551–560.
[10] H.B. Wang, M. Dembo, Y.L. Wang, Substrate flexibility regulates growth and apoptosis of normal but not transformed cells, Am. J. Physiol. Cell Physiol. 279 (2000) 1345–1350.
[11] K. Anselme, L. Ploux, A. Ponche, Cell/material interfaces: influence of surface chemistry and surface topography on cell adhesion, J. Adhes. Sci. Technol. 4243 (2011) 43–64.
[12] M. Ball, D.M. Grant, W.J. Lo, C.A. Scotchford, The effect of different surface morphology and roughness on osteoblast-like cells, J. Biomed. Mater. Res. 86A (2008) 637–647.
[13] A.S. Zeiger, B. Hinton, K.J. Van Vliet, Why the dish makes a difference: quantitative comparison of polystyrene culture surfaces, Acta Biomater. 9 (2013) 7354–7361.
[14] M.P. Lutolf, J.A. Hubbell, Synthetic biomaterials as instructive extracellular microenvironments for morphogenesis in tissue engineering, Nat. Biotechnol. 23 (2005) 47–55.
[15] E.S. Kang, D.S. Kim, I.R. Suhito, W. Lee, I. Song, T.H. Kim, Two-dimensional material-based bionano platforms to control mesenchymal stem cell differentiation, Biomater. Res. 22 (2018) 1–12.
[16] S. Vafaei, S.R. Tabaei, N.J. Cho, Optimizing the performance of supported lipid bilayers as cell culture platforms based on extracellular matrix functionalization, ACS Omega 2 (2017) 2395–2404.
[17] A.M. Ross, H. Nandivada, A.L. Ryan, J. Lahann, Synthetic substrates for long-term stem cell culture, Polymer 53 (2012) 2533–2539.
[18] V. Lecault, M. VanInsberghe, S. Sekulovic, et al., High-throughput analysis of single hematopoietic stem cell proliferation in microfluidic cell culture arrays, Nat. Methods 8 (2011) 581–586.
[19] E.Z. Macosko, A. Basu, R. Satija, J. Nemesh, K. Shekhar, M. Goldman, et al., Highly parallel genome-wide expression profiling of individual cells using nanoliter droplets, Cell 161 (2015) 1202–1214.
[20] S. Mashaghi, A. Abbaspourrad, D.A. Weitz, A.M. van Oijen, Droplet microfluidics: a tool for biology, chemistry and nanotechnology, TrAC - Trends Anal. Chem. 82 (2016) 118–125.
[21] T. Hartung, G. Daston, Are in vitro tests suitable for regulatory use? Toxicol. Sci. 111 (2009) 233–237.
[22] A. Ghallab, H.M. Bolt, In vitro systems: current limitations and future perspectives, Arch. Toxicol. 88 (2014) 2085–2087.
[23] A.A. Popova, S.M. Schillo, K. Demir, E. Ueda, A. Nesterov-Mueller, P.A. Levkin, Droplet-array (DA) sandwich chip: a versatile platform for high-throughput cell screening based on superhydrophobic-superhydrophilic micropatterning, Adv. Mater. 27 (2015) 5217–5222.
[24] A.A. Popova, K. Demir, T.G. Hartanto, E. Schmitt, P.A. Levkin, Droplet-microarray on superhydrophobic-superhydrophilic patterns for high-throughput live cell screenings, RSC Adv. 6 (2016) 38263–38276.
[25] T. Tronser, A.A. Popova, P.A. Levkin, Miniaturized platform for high-throughput screening of stem cells, Curr. Opin. Biotechnol. 46 (2017) 141–149.
[26] H. Cui, X. Wang, J. Wesslowski, T. Tronser, J. Rosenbauer, A. Schug, et al., Assembly of multi-spheroid cellular architectures by programmable droplet merging, Adv. Mater. 16 (2020), e2006434.
[27] A.A. Popova, C. Depew, K.M. Permana, A. Trubitsyn, R. Peravali, J.Á. Ordiano, et al., Evaluation of the droplet-microarray platform for high-throughput screening of suspension cells, SLAS Technol. 22 (2017) 163–175.
[28] T. Tronser, A.A. Popova, M. Jaggy, M. Bastmeyer, P.A. Levkin, Droplet microarray based on patterned superhydrophobic surfaces prevents stem cell differentiation and enables high-throughput stem cell screening, Adv. Healthc. Mater. 6 (2017) 23.
[29] A.A. Popova, S. Dietrich, W. Huber, M. Reischl, R. Peravali, P.A. Levkin, Miniaturized drug sensitivity and resistance test on patient-derived cells using droplet-microarray, SLAS Technol. 13 (2020), 2472630320934432.
[30] A.A. Popova, T. Tronser, K. Demir, P. Haitz, K. Kuodyte, V. Starkuviene, et al., Facile one step formation and screening of tumor spheroids using droplet-microarray platform, Small 15 (2019), e1901299.
[31] L.T. Allen, E.J.P. Fox, I. Blute, Z.D. Kelly, Y. Rochev, A.K. Keenan, et al., Interaction of soft condensed materials with living cells: phenotype/transcriptome correlations for the hydrophobic effect, Proc. Natl. Acad. Sci. U.S.A. 100 (2003) 6331–6336.
[32] J. He, C. Sun, Z. Gu, Y. Yang, M. Gu, et al., Morphology, migration, and transcriptome analysis of Schwann cell culture on butterfly wings with different surface architectures, ACS Nano 12 (2018) 9660–9668.
[33] P. Chandran, J.E. Riviere, N.A. Monteiro-Riviere, Surface chemistry of gold nanoparticles determines the biocorona composition impacting cellular uptake, toxicity and gene expression profiles in human endothelial cells, Nanotoxicology 11 (2017) 507–519.

[34] E.M. Grzincic, J.A. Yang, J. Drnevich, P. Falagan-Lotsch, C.J. Murphy, Global transcriptomic analysis of model human cell lines exposed to surface-modified gold nanoparticles: the effect of surface chemistry, Nanoscale 7 (2015) 1349–1362.
[35] S. Shafaie, V. Hutter, M.B. Brown, M.T. Cook, D.Y.S. Chau, Influence of surface geometry on the culture of human cell lines: a comparative study using flat, round-bottom and v-shaped 96 well plates, PloS One 12 (2017) 1–14.
[36] T. Kasputis, A.K. Pannier, The role of surface chemistry-induced cell characteristics on nonviral gene delivery to mouse fibroblasts, J. Biol. Eng. 6 (2012) 1–11.
[37] G.O. Gey, W.D. Coffman, M.T. Kubicek, Tissue culture studies of the proliferative capacity of cervical carcinoma and normal epithelium, Canc. Res. 12 (1952) 264–265.
[38] W.F. Scherer, J.T. Syverton, G.O. Gey, Studies on the propagation in vitro of poliomyelitis viruses. IV. Viral multiplication in a stable strain of human malignant epithelial cells (strain HeLa) derived from an epidermoid carcinoma of the cervix, J. Exp. Med. 97 (1953) 695–710.
[39] A.L. Svalastog, L. Martinelli, Representing life as opposed to being: the bio-objectification process of the HeLa cells and its relation to personalized medicine, Croat. Med. J. 54 (2013) 397–402.
[40] J.J. Landry, P.T. Pyl, T. Rausch, T. Zichner, M.M. Tekkedil, A.M. Stütz, et al., The genomic and transcriptomic landscape of a HeLa cell line, G3 (Bethesda) 3 (2013) 1213–1224.
[41] F.L. Geyer, E. Ueda, U. Liebel, N. Grau, P.A. Levkin, Superhydrophobic-superhydrophilic micropatterning: towards genome-on-a-chip cell microarrays, Angew. Chem. Int. Ed. 50 (2011) 8424–8427.
[42] W. Feng, L. Li, E. Ueda, J. Li, S. Heißler, A. Welle, et al., Surface patterning via thiol-yne click chemistry: an extremely fast and versatile approach to superhydrophilic-superhydrophobic micropatterns, Adv. Mater. Interfaces. 1 (2014) 1–6.
[43] M. Benz, A. Asperger, M. Hamester, A. Welle, S. Heissler, P.A. Levkin, A combined high-throughput and high-content platform for unified on-chip synthesis, characterization and biological screening, Nat. Commun. 11 (2020) 5391.
[44] M. Benz, M.R. Molla, A. Böser, A. Rosenfeld, P.A. Levkin, Marrying chemistry with biology by combining on-chip solution-based combinatorial synthesis and cellular screening, Nat. Commun. 10 (2019) 1–10.
[45] C.A. Schneider, W.S. Rasband, K.W. Eliceiri, NIH Image to ImageJ: 25 years of image analysis, Nat. Methods 9 (2012) 671–675.
[46] G.J. Hannon, FASTX-toolkit, 2010. http://hannonlab.cshl.edu/fastx_toolkit.
[47] A. Dobin, C.A. Davis, F. Schlesinger, J. Drenkow, C. Zaleski, S. Jha, et al., STAR: ultrafast universal RNA-seq aligner, Bioinformatics 29 (2013) 15–21.
[48] S. Anders, P.T. Pyl, W. Huber, HTSeq-A Python framework to work with high-throughput sequencing data, Bioinformatics 31 (2015) 166–169.
[49] M.I. Love, W. Huber, S. Anders, Moderated estimation of fold change and dispersion for RNA-seq data with DESeq2, Genome Biol. 15 (2014) 1–21.
[50] The Gene Ontology Consortium, M. Ashburner, C.A. Ball, J.A. Blake, D. Botstein, H. Butler, et al., Gene ontology: tool for the unification of biology. The Gene Ontology Consortium, Nat. Genet. 25 (2000) 25–29.
[51] C.C. Chang, M. Wu, F. Yuan, Role of specific endocytic pathways in electrotransfection of cells, Mol. Ther. Methods Clin. Dev. 17 (2014) 14058.
[52] Y.L. Lin, Y. YukselDurmaz, J.E. Nör, M.E. ElSayed, Synergistic combination of small molecule inhibitor and RNA interference against antiapoptotic Bcl-2 protein in head and neck cancer cells, Mol. Pharm. 10 (2013) 2730–2738.
[53] Q. Li, B. Zhang, N. Kasoju, J. Ma, A. Yang, Z. Cui, et al., Differential and interactive effects of substrate topography and chemistry on human mesenchymal stem cell gene expression, Int. J. Mol. Sci. 19 (2018) 2344.
[54] P. Fuentes, M. Sesé, P.J. Guijarro, M. Emperador, S. Sánchez-Redondo, H. Peinado, et al., ITGB3-mediated uptake of small extracellular vesicles facilitates intercellular communication in breast cancer cells, Nat. Commun. 11 (2020) 4261.
[55] M. Muhia, E. Thies, D. Labonté, A.E. Ghiretti, K.V. Gromova, F. Xompero, et al., The kinesin KIF21B regulates microtubule dynamics and is essential for neuronal morphology, synapse function, and learning and memory, Cell Rep. 15 (2016) 968–977.
[56] I. Rubio-Aliaga, C.A. Wagner Ca, Regulation and function of the SLC38A3/SNAT3 glutamine transporter, Channels (Austin) 10 (2016) 440–452.
[57] X. Liu, T. Li, B. Tuo, Physiological and pathophysiological relevance of the anion transporter Slc26a9 in multiple organs, Front. Physiol. 9 (2018) 1197.
[58] I. Carpentier, R. Beyaert, TRAF1 is a TNF inducible regulator of NF-kappaB activation, FEBS Lett. 460 (1999) 246–250.
[59] Y. Liu, F. Echtermeyer, F. Thilo, G. Theilmeier, A. Schmidt, R. Schülein, et al., The proteoglycan syndecan 4 regulates transient receptor potential canonical 6 channels via RhoA/Rho-associated protein kinase signaling, Arterioscler. Thromb. Vasc. Biol. 32 (2012) 378–385.
[60] P. Kesharwani, S. Banerjee, U. Gupta, M.C.I. Mohd Amin, S. Padhye, F.H. Sarkar, et al., PAMAM dendrimers as promising nanocarriers for RNAi therapeutics, Mater. Today 18 (2015) 565–572.
[61] A.M. Caminade, C.O. Turrin, Dendrimers for drug delivery, J. Mater. Chem. B. 2 (2014) 4055–4066.
[62] Y. Omidi, A.J. Hollins, R.M. Drayton, S. Akhtar, Polypropylenimine dendrimer-induced gene expression changes: the effect of complexation with DNA, dendrimer generation and cell type, J. Drug Target. 13 (2005) 431–443.
[63] R. Gras, L. Almonacid, P. Ortega, M.J. Serramia, R. Gomez, F.J. De La Mata, et al., Changes in gene expression pattern of human primary macrophages induced by carbosilane dendrimer 2G-NN16, Pharm. Res. 26 (2009) 577–586.
[64] E.E. Benarroch, Acid-sensing cation channels: structure, function, and pathophysiologic implications, Neurology 82 (2014) 628–635.
[65] K.J. Hatfield, S.L. Bedringsaas, A. Ryningen, B.T. Gjertsen, O. Bruserud, Hypoxia increases HIF-1α expression and constitutive cytokine release by primary human acute myeloid leukaemia cells, Eur. Cytokine Netw. 21 (2010) 154–164.
[66] T.S. Hsu, S.T. Mo, P.N. Hsu, M.Z. Lai, c-FLIP is a target of the E3 ligase deltex1 in gastric cancer, Cell Death Dis. 9 (2018) 135.